SAND--96-8508C

CONF-960772--14

Application of the GRI 1.2 Methane Oxidation Model to Methane and Methanol Oxidation in Supercritical Water

Steven F. Rice

Combustion Research Facility

Sandia National Laboratories, Livermore, CA 94551-0969

Tel: (510) 294-1353

Fax: (510) 294-1004

Email: steve_rice@sandia.gov

submitted to:

Twenty-sixth International Symposium on Combustion

Oral Presentation

Colloquium: General Reaction Kinetics

Word Length

Text:	**3730**
Figures &Table (7):	**1400**
Total:	**5130**

Application of the GRI 1.2 Methane Oxidation Model to Methane and Methanol Oxidation in Supercritical Water

Steven F. Rice

Combustion Research Facility

Sandia National Laboratories, Livermore, CA 94551-0969

Tel: (510) 294-1353

Fax: (510) 294-1004

Email: steve_rice@sandia.gov

submitted to:

Twenty-sixth International Symposium on Combustion

Oral Presentation

Colloquium: General Reaction Kinetics

Abstract

The GRI 1.2 mechanism is used to predict the oxidation rates of methane and methanol by oxygen in supercritical water at 250 bar and temperatures ranging from 420 °C - 630 °C. Using the Chemkin II computational package which assumes an ideal gas equation of state, the GRI model does very well in representing the available experimental results on methane over a wide temperature and concentration range. However, the model may lack key CH_3O_2 reactions needed for a complete description in the <450 °C region. The oxidation of methanol and formation of formaldehyde is not well represented by the GRI mechanism when left unchanged. If two important modifications are made to the reactivity of HO_2, good agreement with the methanol oxidation results is achieved. This paper illustrates that the carefully-assembled GRI 1.2 mechanism, although designed for conventional combustion conditions, can be successfully extended with very little modification to much lower temperature and extreme pressure conditions.

Introduction

Hydrothermal oxidation, and specifically supercritical water oxidation (SCWO), are emerging technologies under development internationally by government laboratories, universities, and private industry for the treatment of hazardous aqueous wastes. SCWO is also suited for treatment of waste materials best handled in water for environmental or safety reasons such as obsolete munitions, rocket motors, and chemical warfare agents. The process is performed at temperatures and pressures above the critical point of water (typically 450 - 650 °C and 250 bar), and is applicable to waste streams containing 0 - 20 percent organics in water. Systems can be designed such that the effluent from waste processing can be evaluated for compliance with applicable discharge regulations before release, ensuring protection of the environment.

An early patent for the process included data showing 99.99% destruction of many normal and halogenated hydrocarbons including tetrachloroethylene, DDT, and PCB [1]. Since then, the number of organic and inorganic chemicals, as well as complex mixtures, treated by SCWO has grown considerably. Industrial wastes have been successfully treated to yield reusable water, clean gases, and inorganic solids [2,3]. Experiments have demonstrated effective destruction of the organic components of a simulated U.S. Department of Energy mixed waste (radioactive plus organic waste) [4]. Other experiments illustrated the applicability of SCWO to wastes characteristic of operations at Naval installations [5]. Recently, this technology has been successfully applied in the commercial chemical industry for

the destruction of petrochemical research waste products [6]. Many other chemicals have been tested in this environment for simple destruction efficiency and other chemical processing applications [7,8].

Despite recent developments, a thorough understanding of the operative chemical kinetics will be required to underpin future applications of supercritical water oxidation technology. For example, shipboard systems will require especially compact equipment and efficient design. The disposal of munitions will require improvements in solids handling and corrosion mitigation. These improvements will not be possible without better predictive models for the time, temperature, density, and concentration dependence of the oxidation process. Predictive models will be needed to design large-scale systems for energy- and cost-efficient operation, assure safety, and manage heat release.

The current understanding of the rates and mechanisms of reactions in supercritical water is limited to a small, but growing, list of empirical global expressions for simple chemicals. However, global expression are of limited use in the formulation of a predictive model of SCWO. To be valuable as design tools, models must be based on at least a detailed quantitative mechanism incorporating the key elementary reaction steps. Some researchers have inferred details of important elementary reactions through experiments on the oxidation of simple compounds that have reaction steps in common with the oxidation of larger hydrocarbons and have used lumping strategies to model more complicated systems. Valuable

progress has been made, but agreement between elementary models and experiments has been only qualitative until very recently. In addition, problems exist in the sparse set of experimental data including a seemingly wide variation in experimental results from different research efforts as a function of feed concentration.

The first attempt to use an elementary reaction model to describe the kinetics of oxidation of simple organics, methane and methanol, in supercritical water was reported by Webley et. al. [9,10]. The approach was to modify a successful kinetic scheme generated for high temperature, gas phase oxidation [11]. Several modifications of this mechanism were included to account for high-density effects on unimolecular reaction rates. The most important modification was to express the unimolecular thermal decomposition rate of H_2O_2 in its high-pressure form, suggested by RRKM calculations [12]. They found that this mechanism successfully reproduced their methanol data, but failed to even approximate the experimental results they had obtained for methane.

Recently, others have developed new more extensive elementary reaction models for the oxidation of methane and methanol in supercritical water. Brock and Savage [13] have presented a model for methane, methanol, hydrogen, and CO oxidation and tested it against results from Tester and coworkers. This model was assembled from a large number of independent investigations on individual reactions. This model make use of the Chemkin II [14] format which assumes an

ideal gas equation of state. In general, agreement with experiment was good for methane and hydrogen, but predictions for methanol and CO were less accurate.

Another similar model, developed by Alkam et. al. [15] and first presented in 1991 by Schmitt et. al. [16] reproduces the earlier methanol results of Tester and coworkers, when the reaction rate constant for $CH_3OH + HO_2$ is reduced [17]. This model runs in the developmental Chemkin Real Gas format [18] which has provisions for nonideal equations of state and automatically makes corrections to reverse reactions rates to account for changes in fugacity coefficients. The advantage of this format, at hydrothermal conditions, is that the density of water in the $0.3\rho_{crit}<\rho<0.8\rho_{crit}$ range is much better represented using the Peng-Robinson equation of state. However, this density range corresponds to a fairly small range of T and P. At densities much lower, the ideal gas equation of state is adequate, and at higher densities, near the critical density, the Peng-Robinson equation of state begins to fail.

Recently, we have completed two sets of experiments on methane and methanol using a Raman spectroscopic method to monitor reaction kinetics [19, 20]. These new experimental results provide a more complete set of data with which the elementary models can be compared. It is particularly important to note that the oxidation rates from 440°C to 500°C at 250 bar reported in Ref. 20 indicate that the oxidation of methanol may be much faster than originally reported and both of these newer models [13,15] will accurately reproduce these data [20].

The goal of this paper is to begin to make the connection between the high - pressure, low-temperature results from recent experiments to the current best effort at representing oxidation of C1 species at combustion conditions. It is important to establish this relationship with the smallest amount of customization as possible, with all of the parameters for both the mechanism and thermodynamics originating from a single well-documented source and the computation conducted in a well-established code. In this paper the application of the recently developed GRI 1.2 mechanism [21] to the oxidation of methane and methanol at 250 bar and 420 - 630 °C is examined. The results from the mechanism applied in the Chemkin II computational package are compared with a variety of experiments on these two fuels. These calculations show that the GRI 1.2 mechanism reproduces almost all experimental results on methane very accurately. In addition, good agreement for fuel consumption and formaldehyde production during methanol oxidation can be obtained with the inclusion of two critical reactions involving HO_2. There are several important observations regarding the reactivity of HO_2 and CH_3O_2 in these systems leading to implications for the extension of the GRI mechanism to lower temperatures when contrasted with the two other mechanisms identified above. In addition, this paper illustrates that in order to compare different experimental results from different sources, the experimental concentration range must be considered.

Results and Discussion

Methods

The GRI 1.2 mechanism is accompanied by a Chemkin-compatible thermodynamic data base. The calculations reported here use this thermodynamic data base. The several calculations reported here using the mechanism of Schmitt/Alkam [15,16] use the GRI thermodynamic data base with the addition of properties for CH_3O_2, and several other less important alkyl peroxides, calculated using THERM [22]. These species are included in the Schmitt/Alkam mechanism, but not in the GRI or Chemkin data base. All calculations are done using the SENKIN driver package [23] at constant pressure and temperature conditions.

The calculations were done at a system pressure of 250 bar over a temperature range of 420°C - 630 °C and assume the ideal gas equation of state for all species, including water. As a result, the number density of water is always lower in the calculation than it would be using an exact equation of state for water. However, changes in the water concentration on the order of 10-20% affect the overall quantitative results very little. It is likely that the error in the water density will become more important below 420 °C at this pressure.

Oxygen is used as the oxidizer at an equivalence ratio of 0.75 for most of the calculations. When oxygen concentration is varied, the equivalence ratio is listed. In the examples where fuel concentration is varied, the oxygen is varied accordingly

to preserve an equivalence ratio of 0.75. Moderately lean conditions such as these are likely to be used in industrial SCWO systems.

Some of the comparison with experiment is done by way of an effective first order rate constant, k_{eff}, defined for the purposes of this paper to be the reciprocal of the time at which the initial fuel mole fraction has fallen to 1/e of is original amount. This permits us to combine the results of experiments and calculations at different temperatures and feed concentrations on a single graph. Unfortunately, this paper simultaneously illustrates that these reactions generally are not first order when the fuel concentration is varied over a wide range. In addition, distinct induction times are typical for these and similar reacting systems [20, 23, 25]. However, the k_{eff} is still the simplest way to represent the reaction rate when comparisons are done for conditions where the rate varies over an order of magnitude.

Methane

Figure 1 shows the results from several calculations for the oxidation of methane at 690, 720, 830, and 900 K. Included on the figure are experimental data from Ref. 9 and Ref. 19. The references contain the details of the experimental methods and data analysis. The results at 0.1 mole/l from T= 390 °C to 440 °C are from a global fit to dozens of experiments at 270 bar at this initial fuel concentration. The reactions in these experiments were followed continuously to approximately 0.01 mole/l. The global fit produced the relationship

$$- d[CH_4]/dt = 10^{17.1} \exp(-30100/T) [CH_4]^{1.84} [O_2]^{-0.06} \qquad (1)$$

where the concentrations are in mole/l and the preexponential factor is chosen so the rate is in mole/l-s. The line marked at 0.003 mole/l is from a calculation using Equation 1, extrapolated to lower concentration. Because the global fit produced an exponent of 1.84 for the fuel concentration, the first order k_{eff} calculated at 0.003 mole/l is less than at 0.1 mole/liter. The experiments covered both lean and rich conditions, but no significant oxygen concentration dependence was observed. In addition, no significant induction period was observed. The experiments reported in Ref. 9 were also conducted at both lean and rich conditions. A global fit to these data gives an expression for the fuel consumption to be

$$- d[CH_4]/dt = 10^{11.1} \exp(-21500/T) [CH_4]^{0.99} [O_2]^{0.66} \qquad (2)$$

The agreement of the Chemkin calculation using the unmodified GRI mechanism with the experimental data is excellent. The calculation did reveal fuel consumption curves that exhibited a brief induction period, which in general was a small fraction of the 1/e time constant. This shows that the GRI 1.2 mechanism can accurately reproduce the available fuel consumption rates for the oxidation of methane over the entire temperature range likely to be used in SCWO applications. The mechanism reproduces the absolute consumption rate and shows a distinct

reaction rate dependence on initial fuel concentration. The experiments show that the low temperature results extrapolate smoothly to data measured at high temperature.

Included on this plot is a similar analysis from the Schmitt/Alkam [15] reaction mechanism. This mechanism systematically predicts rates that are about an order of magnitude faster than is observed. The model presented in Ref. 13, before adjusting parameters to reproduce the experimental data, is more accurate, but still overestimates the reaction rate for methane in the 550°C - 630°C region by about a factor of two. This corresponds to an error in the reaction temperature of 60 K.

Figure 2 shows a qualitative view of the pathway of methane to CO_2 representative of our temperature range. Only a very small fraction of the CH_3O is converted to methanol by reaction with water, so this path does not appear in the figure. In addition, because methanol is significantly more reactive than methane, it is not accumulated. In fact, no significant amount of transient non-radical species are accumulated, other than CO and CO_2. This is in contrast to the results for methanol oxidation where formaldehyde and hydrogen peroxide are produced in significant quantities.

Figure 3 shows a more complicated flux diagram for the oxidation of methane using the Schmitt/Alkam mechanism. The fundamental difference with the GRI mechanism is the rapid equilibrium reaction

$$CH_3 + O_2 + M <=> CH_3O_2 + M \qquad (3)$$

The presence of this reaction dominates the subsequent oxidation chemistry until formaldehyde is reached. The route by which methane is oxidized is very different if this key reaction, and the subsequent reactions of CH_3O_2 as an oxidizer with fuel species, are included. These reactions are not included in the GRI mechanism.

The performance of the GRI mechanism can be evaluated on aspects other than the fuel consumption rates. The Ref. 9 global fit suggests that there is an oxygen concentration dependence of order 0.6. Table 1 shows GRI mechanism predictions for varying the equivalence ratios and a constant fuel mole fraction of 0.0005 at 600 °C. The GRI mechanism shows a clear trend in acceptable agreement with Ref. 9 where the overall rate changes as $[O_2]^{0.6}$. The calculated results fit very accurately to an oxygen concentration exponent of 0.734. However, the GRI mechanism also shows the same O_2 dependence at lower temperature in contrast to the global fit from Ref. 19. The same calculation using the Schmitt/Alkam model shows essentially no dependence on oxygen concentration. This suggests that the GRI

mechanism is not fully representing the additional pathways associated with temperatures below 450°C.

The inclusion of the rapid equilibrium with O_2 in the Schmitt/Alkam model serves to remove any oxygen dependence from the mechanism. It is possible that the GRI mechanism is appropriate at higher temperature, but the methylperoxyl chemistry must be included at lower temperature. The inaccurately high rates calculated at low concentration by the Schmitt/Alkam model in Figure 1 may originate from poor kinetic parameters and thermodynamics for the methylperoxyl chemistry.

Methanol

Significant new results have become available examining the oxidation of methanol and the simultaneous production of formaldehyde [20] permitting a comparison of the GRI mechanism to this system. Figure 4 shows a comparison of the rate of methanol disappearance predicted from the GRI mechanism and the experimental data from Ref. 20. The agreement between the GRI mechanism and the measurements is poor. This is primarily because the mechanism lacks the key reactions

$$CH_3OH + HO_2 => CH_2OH + H_2O_2 \qquad (4)$$

and

$$CH_3OH + O_2 => CH_2OH + HO_2 \qquad (5)$$

The presence of Reaction 5 is not significant at hydrothermal conditions, but without Reaction 4, an unreasonable induction period is calculated. Figure 4 also shows the "GRI-modified" prediction when these steps, and reverse reactions, are added to the scheme with the following parameters used for Reaction 4: A_f = 3.98×10^{13}, Ea_f = 19.4 Kcal/mol, b_f = 0.00, $A_r = 3.13 \times 10^{15}$, Ea_r = 10.75 Kcal/mole, b_r = -0.90; where f and r refer to the forward and reverse reactions. The results appear to be in good agreement. Note that the difference in rate may be almost a factor of two, but in this temperature range, this corresponds to an error in reaction temperature of only about 10 °C.

The GRI mechanism, with Reactions 4 and 5, still does not predict the accumulation of formaldehyde that is observed in this system with peak concentrations appearing about a factor of five below the observed values. This is because the parameters chosen for the reaction

$$CH_2O + HO_2 => CHO + H_2O_2 \qquad (6)$$

are not consistent with the values reported in Baulch et. al. [26]. They produce a rate constant for the removal of formaldehyde that is too fast in the GRI mechanism. Figure 5 shows the results for the formation of formaldehyde as a fraction of the

total amount of feed carbon, as methanol, compared to the prediction from the modified GRI mechanism when the parameters are changed to those in Ref. 26. Significantly better agreement is achieved.

Figure 6 shows the results of the GRI mechanism for the oxidation of methanol over a range of feed concentrations. The data marked "Raman" are determined using the 1/e effective time constant described in this paper. The other data are from experiments using gas chromatography analysis from samples with reaction times of approximately 7 seconds. The mechanism represents fairly well the change in effective rate constant for feeds of low and high fuel concentration. It also shows the apparent decrease in this effect as temperature is raised, although the agreement on this point is only qualitative.

Conclusion

The recently developed GRI 1.2 methane oxidation mechanism has been applied to the oxidation of methane and methanol by oxygen in water at 250 bar and temperatures ranging from 420 - 630 °C. These conditions deviate substantially from the much higher temperature and lower pressure conditions at which it was designed and optimized. The results for the oxidation of methane with no modification of the mechanism agree very well with the available experimental results at these conditions. However, there is some evidence that the mechanism may be incomplete when applied to the <450 °C range; perhaps because the GRI mechanism does not contain CH_3O_2 chemistry. Aspects of recently developed

mechanisms that contain this chemistry may be required to properly represent oxygen dependence of the lowest temperature methane oxidation data. To represent properly the oxidation of methanol and the formation of formaldehyde, two modifications to the mechanism were required. With these two simple modifications, good agreement was achieved in the temperature range of 440°C to 500 °C.

Acknowledgments

This work was supported by the DoD/DOE/EPA Strategic Environmental Research and Development Program (SERDP). I wish to thank W.J. Pitz (LLNL) and P.B. Butler (University of Iowa) for many useful discussions and for providing the details of their groups' models in advance of publication. I also wish to thank R.R. Steeper, C.M. Griffith (Princeton University) and Åsa C. Rydén (Lund University) for technical assistance.

References

1. Modell, M., U.S. Patent 4,543,190, September 24, 1985.
2. Modell, M. in *Standard Handbook of Hazardous Waste Disposal* (H.M. Freeman, Ed.), McGraw Hill, New York, 1989; pp. 8.153-8.168
3. Barner, H.E., Huang, C. Y., Johnson, T., Martch, M.A., and Killilea, W.R., *J. Hazard. Mater.* 31:1-17 (1992).
4. Bramlette, T.T., Mills, B.E., Hencken, K.R., Brynildson, M.E., Johnston, S.C., Hruby, J.M., Feemster, H.C., Odegard, B.C., and Modell M., *Destruction of*

DOE/DP Surrogate Wastes with Supercritical Water Oxidation Technology, Sandia National Laboratories Report No. SAND90-8229, 1990.

5. Rice, S.F., Steeper, R.R. , LaJeunesse C.A., *Destruction of Representative Navy Wastes Using Supercritical Water Oxidation*, Sandia National Laboratories Report No. SAND94-8203, 1994 and Rice S.F., and Steeper, R.R. submitted to *Journal of Advanced Oxidation Technologies* 1995.

6. Stadig, W.P. *Chemical Processing* , August 1995 pp. 34-39.

7. Tester, J.W., Holgate, H.R., Armellini, F.J., Webley, P.A., Killilea, W.R., Hong, G.T., and Barner, H.E., in *Emerging Technologies in Hazardous Waste Management III* (D.W. Tedder,. and F.G. Pohland, Eds.) American Chemical Society, Washington, DC, 1991; Vol. 518, p. 35.

8. Savage, P.E, Gopalan, S., Mizan, T.I., Martino, C.J., and Brock, E.E., *AICHE Journal* 41:1723-1778 (1995).

9. Webley, P.A., and Tester, J.W.,*Energy & Fuels* 5:411-419 (1991).

10. Webley, P.A., and Tester, J.W., in *Supercritical Fluid Science and Technology* (K.P. Johnston and J.M.L Penninger, Eds.), American Chemical Society, Washington, DC, 1989, Vol. 406, p.259.

11. Warnatz, J., *Twentieth Symposium (International) on Combustion* The Combustion Institute, Pittsburgh, 198, pp. 845-856.

12. Tsang, W., and Hampson, R.F., *J. Phys. Chem. Ref. Data* 15:1087-1279 (1986).

13. Brock E.E., and Savage P.E., *AICHE Journal*, 41:1874-1888 (1995).

14. Kee, R.J., Rupley, F.M., and Miller, J.A., *CHEMKIN-II: A Structured Approach to the Computational Modeling of Chemical Kinetics and Molecular Transport in Flowing Systems* Sandia National Laboratories Report No. SAND89-8009B, 1986.

15. Alkam, M.K., Pai, V.M., Butler, P.B., and Pitz, W.J *in press Combust. Flame* 1996.

16. Schmitt, R.G., Butler, P.B., Bergan, N.E., and Pitz, W.J., and Westbrook, C.K, 1991 Fall Meeting of the Western States Section/The Combustion Institute, University of California at Los Angeles, CA, 1991.

17. Tester, J.W., Webley, P.A., and Holgate, H.R., *Ind. Eng. Chem. Res.*, 32:236-239 (1993).

18. Schmitt, R.G., Butler, P.B., French, N.,B., University of Iowa Report No. UIME PBB 93-006, 1993.

19. Steeper, R.R., Rice, S.F., Kennedy, I.M., and Aiken, J.D., *in press J. Phys. Chem.* 1996.

20. Rice, S.F., Hunter, T.B., Hanush, R.G., and Ryden, A.C., submitted to *Ind. Eng. Chem. Res.*, 1995.

21. Frenklach, M., Wang, H., Yu, C.-L., Goldenberg, M., Bowman, C.T., Hanson, R.K., Davidson, D.F., Chang, E.J., Smith, G.P., Golden, D.M., Gardiner, W.C., and Lissianski, V., found at Web page http://www.gri.org. These results were also presented at 1994 Combustion Symposium Poster, 'An Optimized Kinetics Model for for Natural Gas Combustion', 25th International Symposium on Combustion,Irvine, California, Work-In-Progress Poster Session 3, Number 26 .

22. Ritter, E.R., and Bozzelli, J.W., *Int. J. Chem. Kinet.* 23:767-778 (1991), and W.J. Pitz private communication.

23 Hunter, T.B., Hanush, R.G., and Rice S.F., submitted to *Industrial and Engineering Chemistry Research,* 1995.

24. Lutz, A.E., Kee, R.J., and Miller, J.A., SENKIN: *A Fortran Program for Prediciting Homogeneous Gas Phase Chemical Kinetics with Sensitivity Analysis* Sandia National Laboratories Report No. SAND87-8248, 1988.

25. Meyer, J.C., Marrone, P.A., Tester, J.W., *AICHE Journal* 41:2108 -2121 (1995).

26. Baulch, D.L., Cobos, C.L., Cox, R.A., Esser, C., Frank, P., Just, Th., Kerr, K.A, Pilling, M.J., Troe, J., Walker, R.W., and Warnatz, J., *J. Phys. Chem Ref. Data* 21: 411-734 (1992).

Table 1

Effect of Oxygen Concentration on Rate of Methane Oxidation[a]

O_2 mole fraction	Equivalence ratio	k_{eff} (s^{-1})[b]	Fitted k_{eff} (s^{-1})[c]
0.0133	0.075	0.256	0.294
0.00665	0.15	0.182	0.176
0.00400	0.25	0.132	0.121
0.00266	0.375	0.102	0.090
0.00133	0.75	0.0571	0.0542
0.00100	1.0	0.0438	0.0439
0.00067	1.5	0.0284	0.0327

a - Initial methane mole fraction $=5.0 \times 10^{-4}$, T=600 °C, P=250 bar

b - Defined as $k_{eff} = 1/\tau$, with reaction time, τ, at $[CH_4]/[CH_4]_o = 1/e$.

c -Prediciton from fit to $k_{eff} = a\ (O_2 \text{ mole fraction})^b$, with a= 7.018 and b=0.734

Figure Captions

Figure 1 Comparison of calculated effective first order rate constants for the oxidation of methane from the GRI 1.2 mechanism and experimental results from Ref. 9 and Ref. 19. Also included are the predictions from Ref. 15. The overlap between the calculated rate from Ref. 15 at low concentration with the measured high concentration rates is coincidental.

Figure 2 Flux diagram of the formation and consumption pathways of the major carbon species in the oxidation of CH_4 at 500 °C and 250 bar in supercritical water predicted by the GRI 1.2 mechanism.

Figure 3 Flux diagram of the formation and consumption pathways of the major carbon species in the oxidation of CH_4 at 500 °C and 250 bar in supercritical water predicted by the mechanism described in Alkam et. al. [15].

Figure 4 Comparison of experimental results from Ref. 20 of methanol oxidation at 450 °C and 500 °C at 250 bar with the predictions from the GRI 1.2 mechanism with and without the modifications to HO_2 + CH_3OH and $HO_2 + CH_2O$.

Figure 5 Comparison of experimental results from Ref. 20 for the production of formaldehyde during methanol oxidation at 450 °C and 500 °C at 250 bar with the predictions from the GRI 1.2 mechanism with the

modifications to HO_2 + CH_3OH and HO_2 + CH_2O. The expression $[CH_2O]/[CH_3OH]_0$ refers to the concentration of formaldehyde observed over the initial methanol feed concentration.

Figure 6 Comparison of the concentration dependence of methanol oxidation with experiments from Ref. 20. Because the temperature varies in this data set, concentration at reaction conditions is not constant. The concentrations reported are ambient temperature feeds concentrations for both the experimental and the calculated values, for consistency. The volumetric concentrations at temperature and 250 bar are significantly less, but may be calculated by an using an equation of state for water. For, example, at 500 °C and 250 bar the density of water is 0.0899 g/cm^3, yielding reaction concentrations about a factor of 11 lower than the feed concentrations. The mole fractions remain constant.

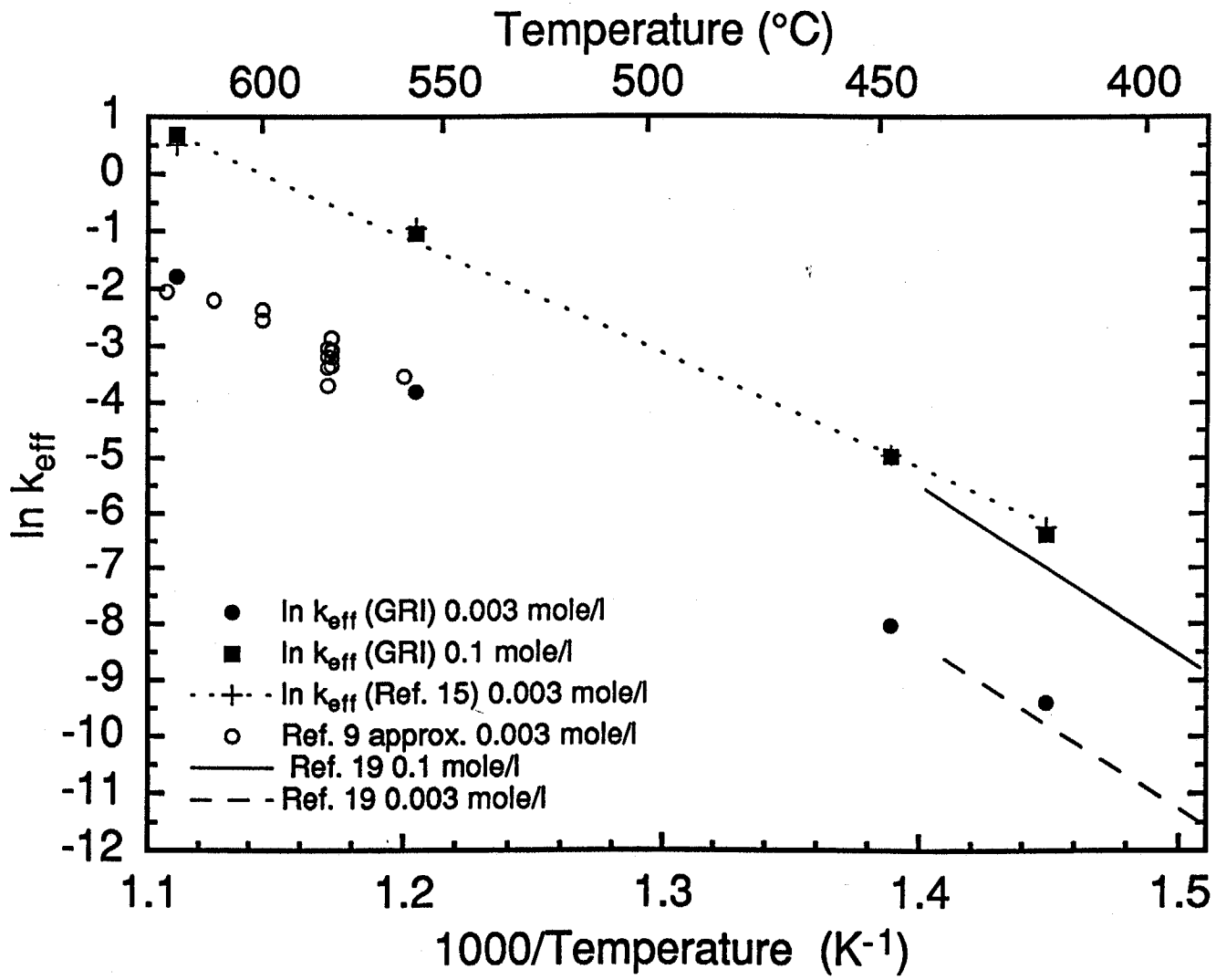
Temperature (°C)
600
550
500
450
400
1
0
-1
-2
-3
-4
-5
-6
-7
-8
-9
-10
-11
-12
ln k_{eff}
1.1
1.2
1.3
1.4
1.5
1000/Temperature (K^{-1})
ln k_{eff} (GRI) 0.003 mole/l
ln k_{eff} (GRI) 0.1 mole/l
ln k_{eff} (Ref. 15) 0.003 mole/l
Ref. 9 approx. 0.003 mole/l
Ref. 19 0.1 mole/l
Ref. 19 0.003 mole/l

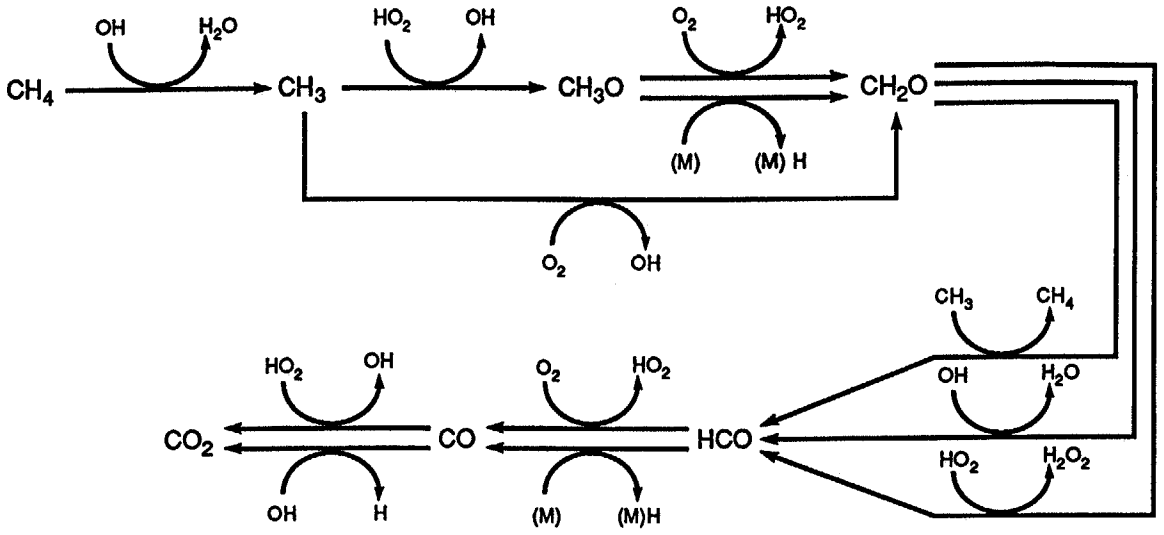
CH4
OH
H2O
CH3
HO2
OH
CH3O
O2
HO2
(M)
(M) H
CH2O
O2
OH
CH3
CH4
OH
H2O
HO2
H2O2
HO2
OH
O2
HO2
CO2
CO
HCO
OH
H
(M)
(M)H

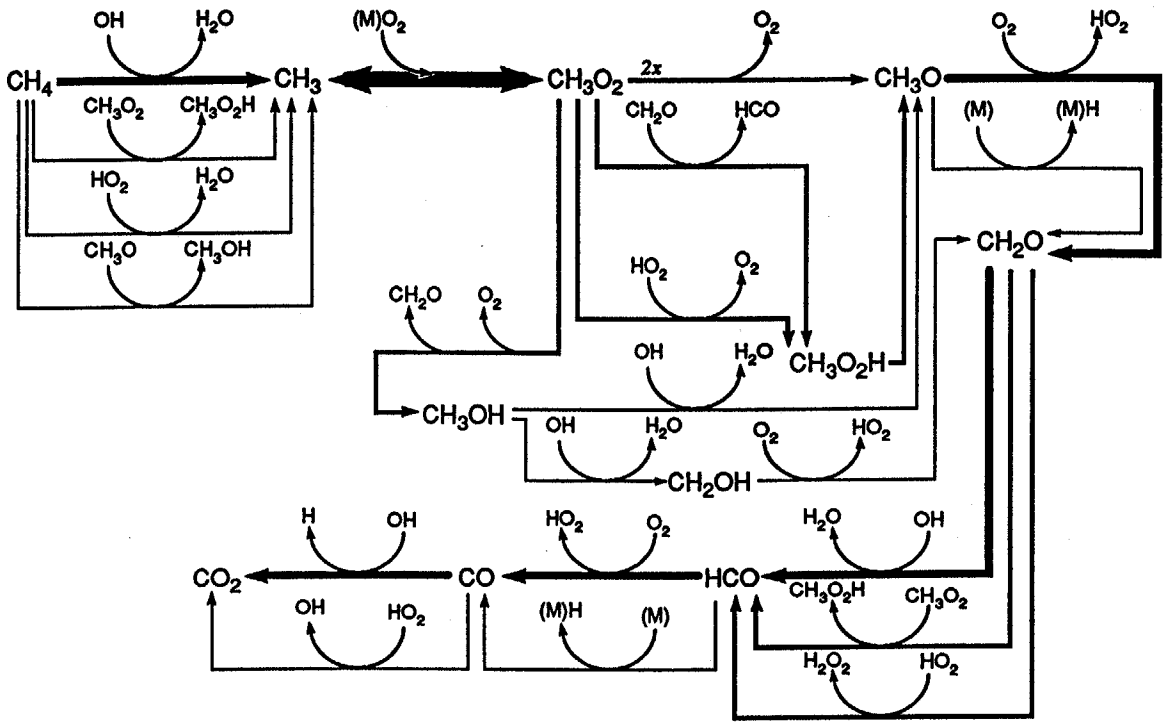
CH4
CH3
CH3O2
CH3O
CH2O
CH3O2H
CH3OH
CH2OH
CO
CO2
HCO
OH
H2O
(M)O2
O2
HO2
2x
CH2O
HCO
(M)
(M)H
H
CH3O2
CH3OH
H2O2

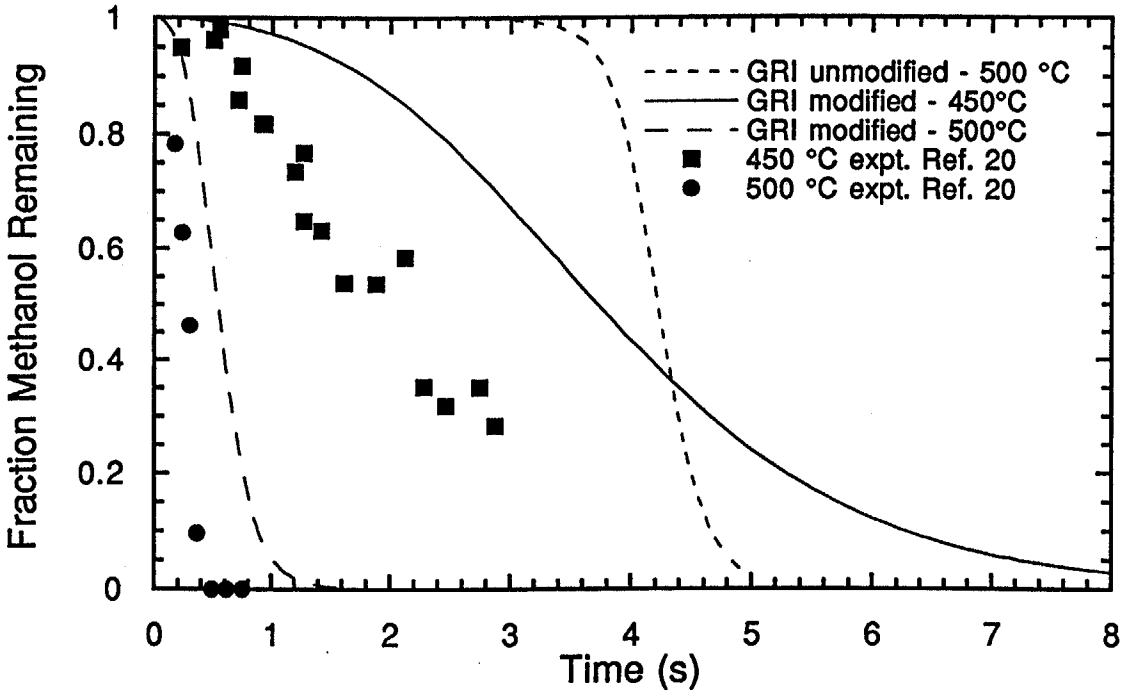
Fraction Methanol Remaining
Time (s)
GRI unmodified - 500 °C
GRI modified - 450°C
GRI modified - 500°C
450 °C expt. Ref. 20
500 °C expt. Ref. 20
0
0.2
0.4
0.6
0.8
1
0
1
2
3
4
5
6
7
8

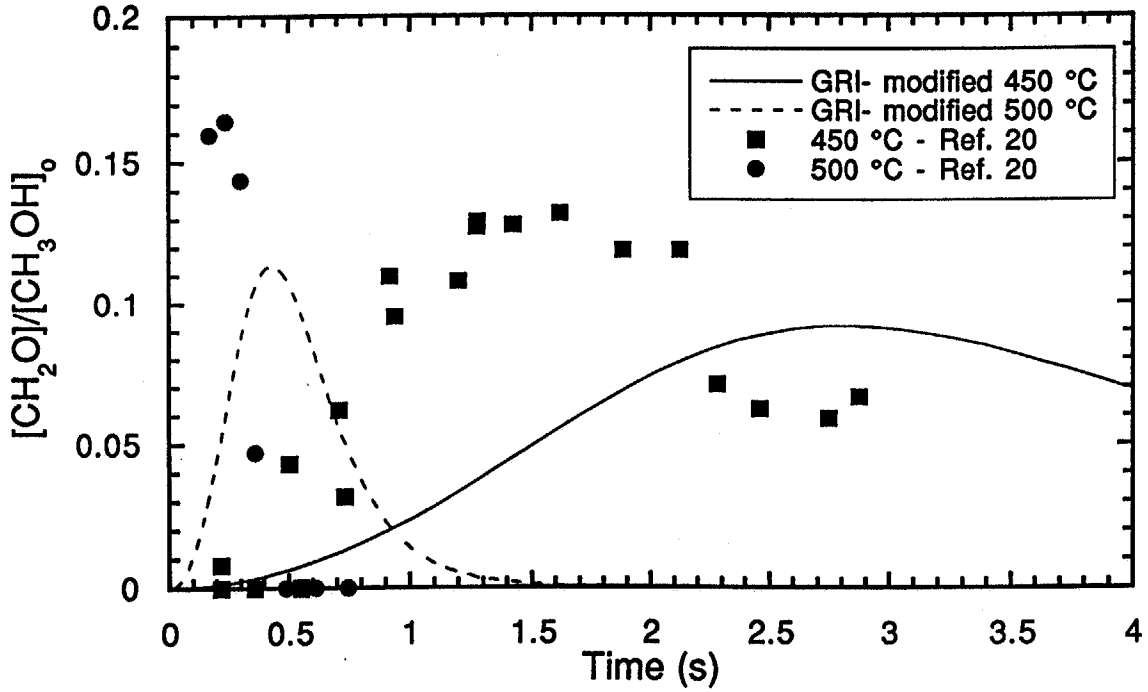
0.2
0.15
0.1
0.05
0
0
0.5
1
1.5
2
2.5
3
3.5
4
Time (s)
[CH2O]/[CH3OH]o
GRI- modified 450 °C
GRI- modified 500 °C
450 °C - Ref. 20
500 °C - Ref. 20

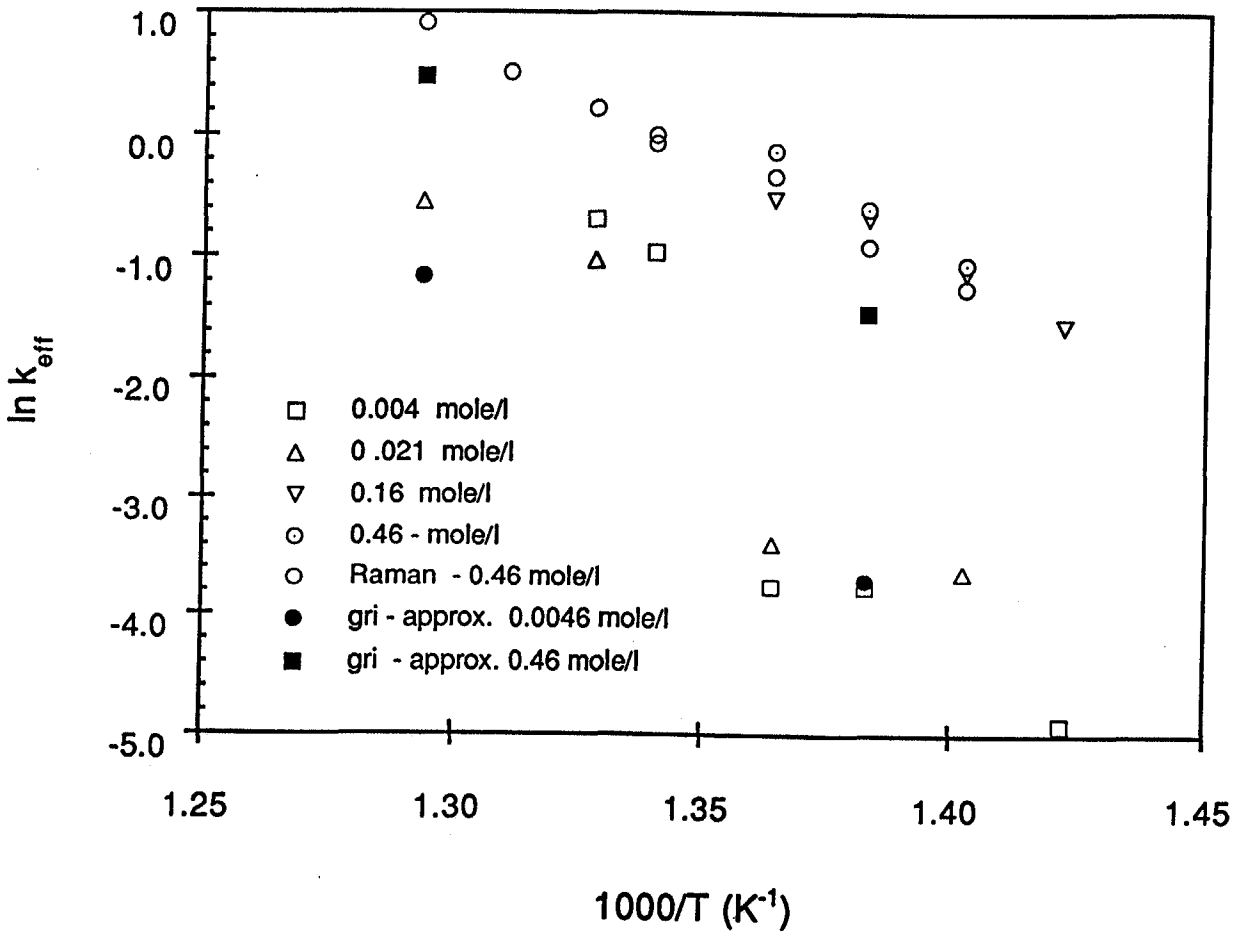
1.0
0.0
-1.0
-2.0
-3.0
-4.0
-5.0
ln k_eff
1.25
1.30
1.35
1.40
1.45
1000/T (K^-1)
0.004 mole/l
0 .021 mole/l
0.16 mole/l
0.46 - mole/l
Raman - 0.46 mole/l
gri - approx. 0.0046 mole/l
gri - approx. 0.46 mole/l